

Controlled synthesis and facets-dependent photocatalysis of TiO₂ nanocrystals

This content has been downloaded from IOPscience. Please scroll down to see the full text.

2015 Semicond. Sci. Technol. 30 044005

(<http://iopscience.iop.org/0268-1242/30/4/044005>)

View [the table of contents for this issue](#), or go to the [journal homepage](#) for more

Download details:

IP Address: 203.110.243.21

This content was downloaded on 06/03/2015 at 11:14

Please note that [terms and conditions apply](#).

Invited Article

Controlled synthesis and facets-dependent photocatalysis of TiO₂ nanocrystals

Nitish Roy¹, Yohan Park², Youngku Sohn² and Debabrata Pradhan¹¹Materials Science Centre, Indian Institute of Technology, Kharagpur 721 302, India²Department of Chemistry, Yeungnam University, Gyeongsan, Gyeongbuk 712-749, KoreaE-mail: deb@matsc.iitkgp.ernet.in

Received 4 September 2014, revised 5 January 2015

Accepted for publication 27 January 2015

Published 5 March 2015



CrossMark

Abstract

Titanium dioxide (TiO₂) is a wide band gap semiconductor that has been extensively used in several environmental applications including degradation of organic hazardous chemicals, water splitting to generate hydrogen, dye sensitized solar cells, self cleaning agents, and pigments. Herein we demonstrate the synthesis of TiO₂ nanocrystals (NCs) with the shapes of ellipsoids, rods, cuboids, and sheets with different exposed facets using a noncorrosive and nontoxic chemical (i.e. diethanolamine) as the shape controlling agent, unlike hydrofluoric acid commonly used. The TiO₂ NCs of diverse shapes with different exposed facets were tested for photocatalytic hydroxyl radical (OH[•]) formation, which determines their photocatalytic behavior and the results were compared with the standard P-25 Degussa. The formation rate of OH[•] per specific surface area was found to be >6 fold higher for rod-shaped TiO₂ NCs than that of commercial Degussa P25 catalyst. The highest photocatalytic activity of rod-shaped TiO₂ NCs is ascribed to the unique chemical environment of {010} exposed facets which facilitates the electron/hole separation in presence of {101} facets.

Keywords: titanium dioxide, photocatalysis, nanocrystals

(Some figures may appear in colour only in the online journal)

1. Introduction

Tailored synthesis of titanium dioxide (TiO₂) nanocrystals (NCs) attracts attention due to their exposed facets dependent photocatalytic properties [1, 2]. In recent years, efforts have been focused on the growth of TiO₂ NCs with {001} exposed facets due to their unique surface chemistry and high surface energy [3, 4]. The NCs with {001} exposed facets are generally prepared using hydrofluoric acid (HF), a very corrosive chemical [3, 5]. Several studies have been subsequently reported on the synthesis of TiO₂ NCs with high-energy {001} exposed facets utilizing HF and/or F-containing titanium salt [6–8]. Moreover, a few studies have recently employed F-free methods to synthesize TiO₂ NCs with {001} exposed facets [9, 10]. The principal reason behind the synthesis of TiO₂ NCs with {001} exposed facets is due to their high reactivity and higher adsorption toward small organic molecules including

water [11], alcohols [12], and acids [13]. However, recent experimental findings contradict the effective and only role of high-energy {001} exposed facets [14–16]. In fact, Selloni *et al* showed poor photocatalysis of ultrathin TiO₂ NCs with virtually {001} exposed facets [17]. In addition, the role of another high-energy facet (i.e. {010}) is ambiguous. Theoretical studies revealed that {010} facets could be more active towards the charge separation in the presence of low-energy {101} facets [18, 19]. This prompts us to investigate the role of high-energy {010} facets along with low-energy {101} facets towards charge separation and thereby the photocatalytic performance. In this study, we demonstrate the role of different exposed facets in the photocatalysis using different shape TiO₂ NCs such as nanoellipsoids, nanosheets, nanorods, nanocapsules, and nanocuboids.

Anatase and rutile, two polymorphs of TiO₂ are different in their crystal structure. Therefore, both have different

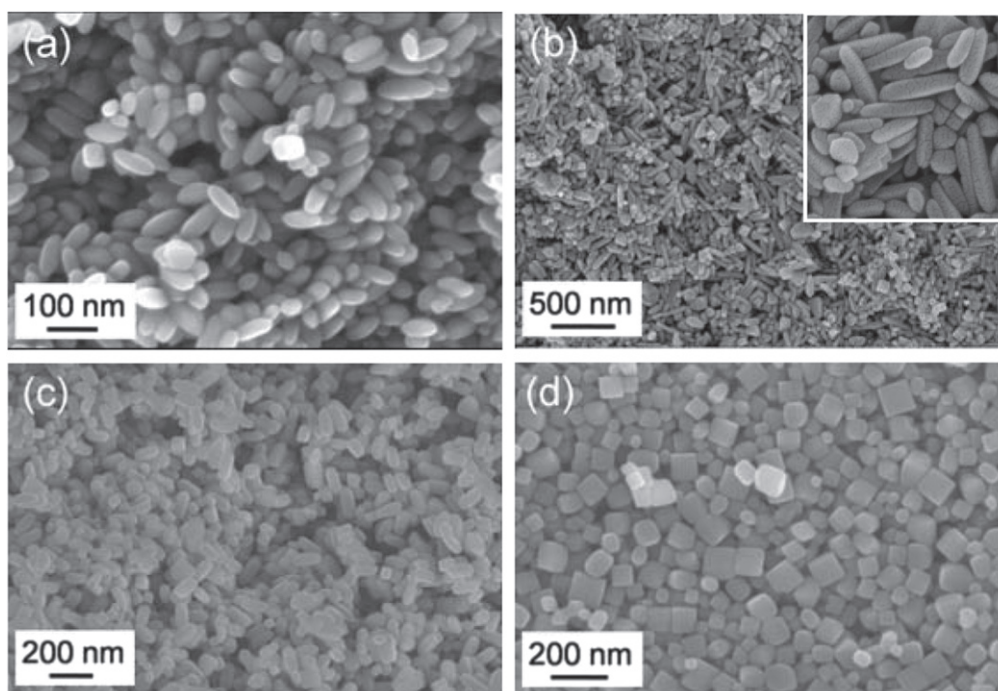


Figure 1. FESEM images of TiO_2 NCs synthesized at different mol ratio of TBAH and DEA at 225°C for 24 h by hydrothermal method using 3 mmol of TTIP as Ti precursor. (a) TBAH:DEA = 10:1, ellipsoid-shaped TiO_2 NCs, (b) TBAH:DEA = 1:1, rod-shaped TiO_2 NCs, (c) TBAH:DEA = 1:2, capsule-shaped TiO_2 NCs, (d) TBAH:DEA = 2:5, cuboid-shaped TiO_2 NCs.

surface and stereochemistry providing difference in electronic, chemical, and physical properties [20]. The difference in electronic states of anatase and rutile is utilized as photoexcited electron/hole separation. This is due to the fact that higher energy of conduction band minima of anatase than the rutile facilitates charge separation at the junction of two mixed phases [21]. The higher activity of the faceted NCs could be due to the difference in electronic states that can be obtained in a single crystal with different exposed facets with different surface and stereochemistry [19, 22]. This leads to difference in reactivity of crystal facets of TiO_2 towards the foreign molecules [14, 23]. The faceted TiO_2 NCs have therefore been studied in detail by both theoretical and experimental works for enhanced photocatalysis [24]. The quantum yield of the faceted TiO_2 NCs is found to be enhanced by suitable manipulation of exposed crystal planes under UV light irradiation [19, 23]. The enhanced quantum yield is ascribed to the preferential flow of photoexcited electrons and holes in the faceted TiO_2 NCs. This is due to the difference in electronic states of different facets and thereby facile photoexcited charge separation in a crystal with two different exposed crystal facets in an optimum ratio [15].

2. Experimental section

2.1. Synthesis of TiO_2 NCs

TiO_2 NCs with different shapes were synthesized using hydrothermal method. Nanoellipsoids were synthesized using 3 mmol (1 mL) of titanium tetraisopropoxide (TTIP) as Ti

precursor, 200 mmol (52 mL) of tetrabutylammonium hydroxide (TBAH) in 0.1 N aqueous as the bridging ligand and 20 mmol (2 mL) of diethanolamine (DEA) as the shape controller. The mixture of the above solution was taken in a Teflon-lined stainless steel autoclave and heated at 225°C for 24 h. Nanorods were synthesized by taking 200 mmol of TBAH (52 mL) and 200 mmol (20 mL) of DEA keeping the precursor quantity (1 mL) and other parameters fixed. Similarly, nanocapsules, nanocuboids, and nanosheets were synthesized by taking 100 (26 mL), 100 (26 mL), 20 mmol (5 mL) of TBAH and 200 (20 mL), 250 (25 mL), 200 (20 mL) mmol of DEA, respectively. After the hydrothermal heat treatment, the autoclave was brought down to room temperature and the product was collected by centrifuging. The white color product was washed with dilute HCl, water, and ethanol, and finally dried in vacuum at 60°C . The dried product was then calcined at 500°C for 2 h to remove the remaining organic residues bound onto the NC's surface. The surface morphology of the samples was characterized by Carl Zeiss SUPRA field emission scanning electron microscope (FESEM). The transmission electron microscopy study was performed using a TECNAI G2 (FEI) or JEM—2100 (JEOL) transmission electron microscope (TEM) operated at 200 kV.

2.2. Photocatalytic testing

Photocatalytic testing was performed taking terephthalic acid (TA) as probe molecule. 2 mM 80 mL aqueous TA was taken and then 20 mg of calcined catalyst was added and sonicated in the dark for 30 min. After sonication of the catalyst-TA solution, it was irradiated under 6 Watt UV light source. The

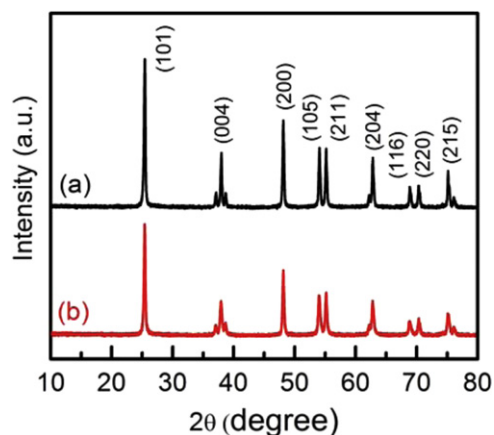


Figure 2. (a) XRD patterns of the sample prepared at TBAH:DEA = 1:1 and (b) 1:10 mol ratio with hydrothermal reaction duration of 24 h at 225 °C using 3 mmol TTIP as precursor.

Table 1. Crystallite size of different NCs in nm measured using Scherrer formula.

Morphology	(101)	(001)	(100)
Ellipsoid	53	51	36
Rod	44	43	33
Capsule	47	41	37
Cuboid	44	36	36
Sheet	21	18	21

reaction mixture was kept 10 cm away from the light source and in each 30 min of interval, 5 mL of the reaction mixture was taken out, the catalyst was removed by centrifuge at 10 000 rpm for 10 min, and then fluorescence emission was measured.

3. Results and discussion

Figure 1 shows the surface morphology of the powder synthesized at various TBAH:DEA mol ratios. The surface morphology of the samples is found to be uniform in nature. The length and diameter of ellipsoid-shaped nanoparticles prepared at mol ratio of TBAH:DEA = 200:20 (10:1) are measured to be 100–150 nm and 60–90 nm, respectively (figure 1(a)). Figure 1(b) shows the rod-like TiO₂ NCs, obtained at a molar ratio of TBAH:DEA = 200:200 (1:1). The length and diameter of the nanorods varies in the range of 200–400 nm and 50–120 nm, respectively. Figure 2(c) shows the capsule-shaped TiO₂ NCs synthesized at TBAH:DEA = 100:200 (1:2) mol ratio, keeping the other reaction parameters (temperature, reaction duration, and precursor quantity) fixed. The length and width of the nanocapsules varies in the range of 150–200 nm and 100–120 nm, respectively. With TBAH:DEA = 100:250 (2:5) mol ratio, cuboid shape of TiO₂ NCs are obtained with size ~150 nm along their diagonal (figure 1(d)). This suggests that the mol ratio of TBAH and DEA has a significant effect on the shape and size of the TiO₂

NCs. Although, the morphology changes upon varying in the mol ratio of DEA and TBAH, cuboid NCs are found along with rod-like and capsule-like TiO₂ NCs. In particular, ~30% and ~35% of cuboid NCs are found to be formed with rod-like and capsule-like TiO₂ NCs, respectively. This is due to partial capping of NCs by smaller quantity of DEA used for the synthesis of rod-like and capsule-like TiO₂ NCs. At higher DEA concentration, the efficient capping of the NCs leads to 100% cuboid NCs for the case of DEA:TBAH 5:2.

Crystallographic phase analysis was carried out using a PANalytical high resolution powder x-ray diffractometer (HRXRD) (PW 3040/60) operated at 30 mA and 40 kV using Cu K α x-rays. Figure 2 shows the powder HRXRD pattern of rod-like and sheet-like TiO₂ NCs synthesized at TBAH:DEA = 1:1 and 1:10 mol ratio, respectively, keeping the other reaction parameters fixed. The Bragg's peaks of the TiO₂ NCs matched the reference pattern (JCPDS 00-002-0387) confirming the pure anatase phase with tetragonal crystal system [20]. No additional peaks revealed that the samples do not contain any crystalline impurities. The intensity ratio of (004) and (200) crystal plane peaks, i.e. $I_{(004)}/I_{(200)}$ for rod-shaped TiO₂ NCs (0.64) is found to be higher than that of sheet-like TiO₂ NCs (0.48) suggesting the major crystal growth along *c*-axis for the rod-shaped TiO₂ NCs [25]. The average crystallite sizes are measured using Scherrer equation taking full-width-half-maximum of major diffraction planes and are shown in table 1. The average crystallite size of the sheet type NCs is found to be much smaller (~20 nm) than the other shapes of NCs (~35 to 50 nm).

The precise size and different exposed planes (facets) of the TiO₂ NCs are characterized in detail using the TEM and high resolution TEM (HRTEM). Figure 3 shows the TEM and HRTEM images of ellipsoid-shaped TiO₂ NCs obtained with TBAH:DEA 10:1 at 225 °C for 24 h using 3 mmol TTIP as precursor. The ellipsoid-shaped TiO₂ NCs are found to be monodisperse and their size distribution is uniform in nature. The length and diameter of these ellipsoid-shaped NCs varies in the range of 100–200 nm and 70–120 nm, respectively (figure 3(a)). Figure 3(b) shows the HRTEM image of the elliptical end showing the lattice fringes. The lattice fringes are measured to be 0.47 and 0.35 nm with an angle of 68° confirming the (002) and (101) plane, respectively, along [100] zone axis [26]. The HRTEM analysis also reveals that the sides of the ellipsoids at the elliptical end are with low-energy {101} exposed facets.

Figure 4 shows the TEM images of rod and capsule-shaped TiO₂ NCs. The length and width of the nanorods (and nanocapsules) varies in the range of 300–600 nm (and 200–350 nm) and 100–200 nm (and 150–250 nm), respectively. Figure 4(b) and its inset show the magnified TEM and HRTEM image, respectively. The lattice fringes are measured to be 0.35 nm matching the (101) planes of anatase TiO₂ [26]. The angle between the trunk of the nanorod and its bent head as marked by a red colored line in figure 4(b), is found to be ~22°, thereby suggesting the {010} exposed facets in the middle portion of the rod while its bent head is with {101} exposed facets. Figure 4(c) shows the TEM image of capsule-shaped TiO₂ NCs obtained with TBAH:DEA = 1:2 mol ratio.

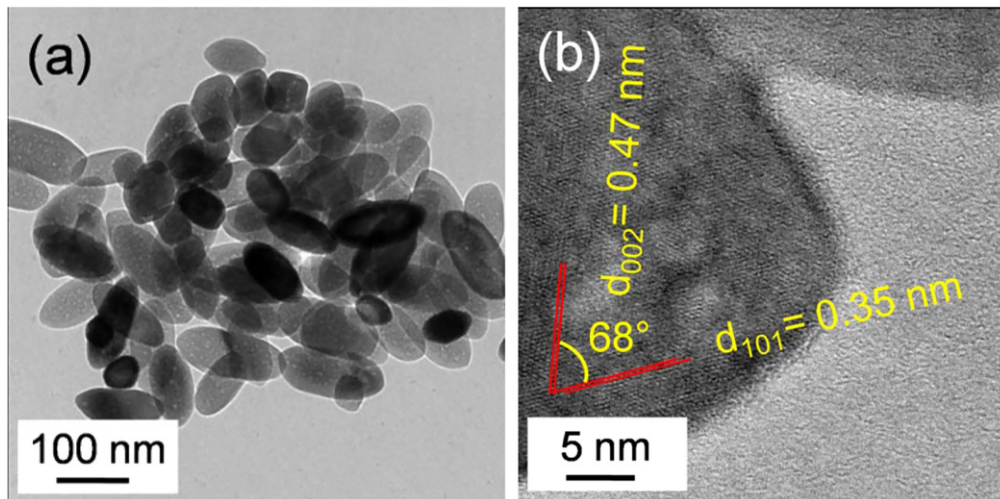


Figure 3. (a) TEM and (b) HRTEM images of ellipsoid-shaped TiO_2 NCs obtained with TBAH:DEA mol ratio of 10:1 and 3 mmol TTIP at 225 °C for 24 h hydrothermal reaction duration.

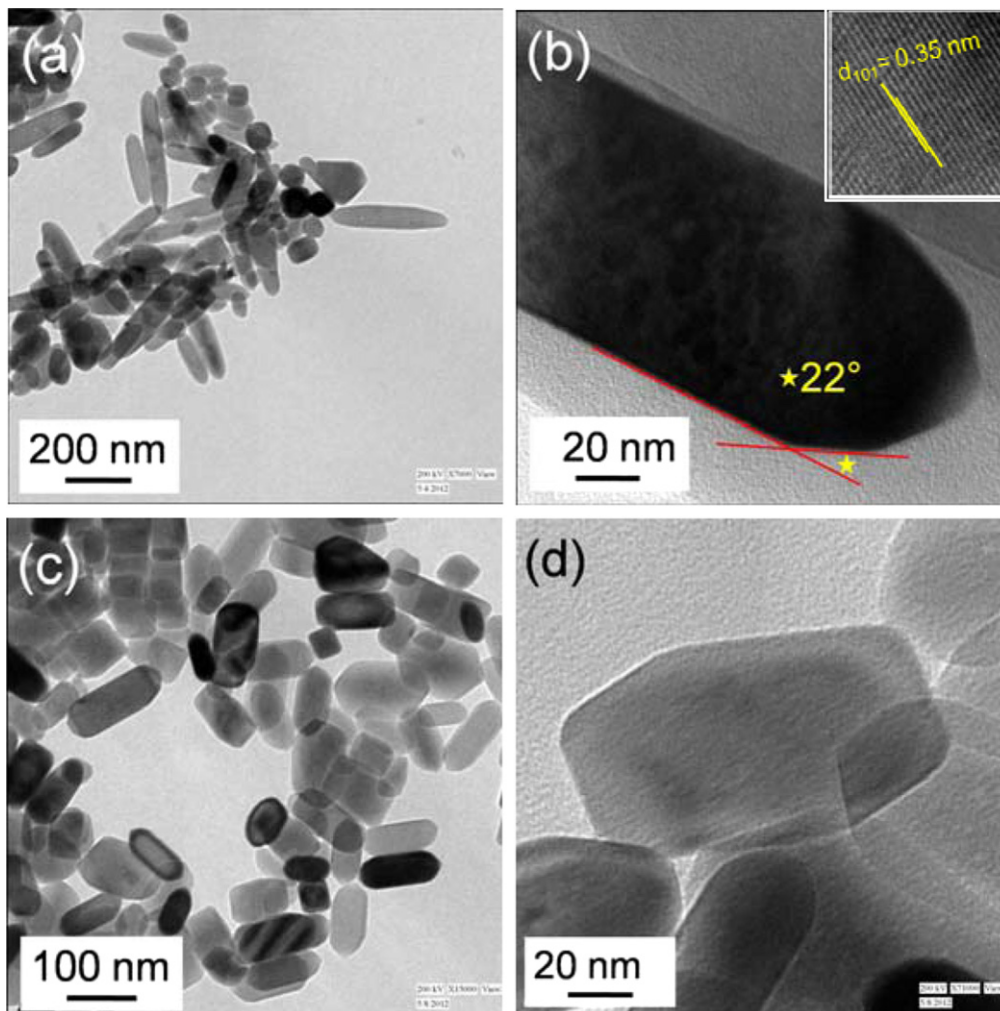


Figure 4. (a) TEM and (b) magnified TEM images of rod-shaped TiO_2 NCs obtained with TBAH:DEA = 1:1. Inset of (b) shows the corresponding HRTEM image. (c), (d) TEM images of capsule-shaped TiO_2 NCs obtained with TBAH:DEA = 1:2.

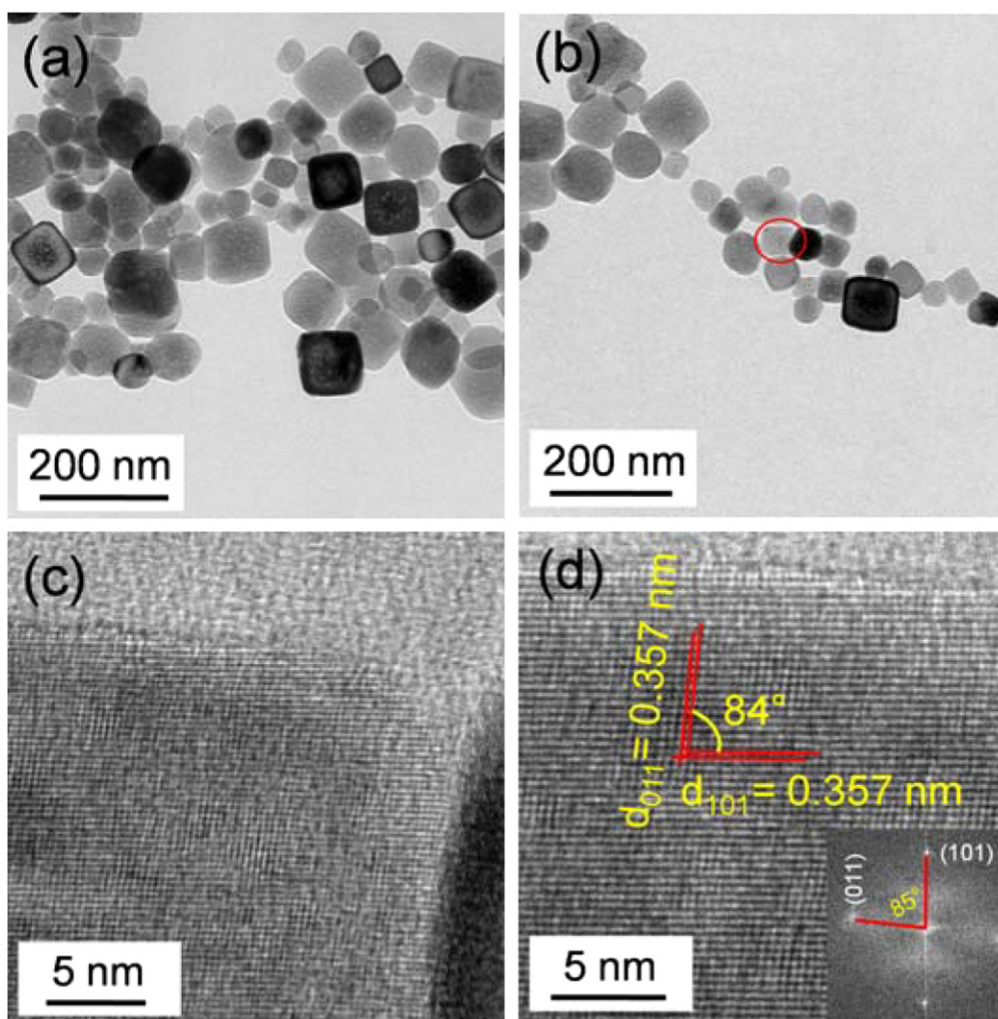


Figure 5. (a), (b) TEM and (c), (d) HRTEM images of cuboid-shaped TiO_2 NCs obtained with TBAH:DEA mol ratio of 2:5 at 225°C for 24 h.

Figure 4(d) shows that different facets of capsule-shaped TiO_2 NCs are orthogonally aligned to each other suggesting the top and bottom of the capsule with $\{001\}$ facets and sides of the body with $\{010\}$ facets.

Figure 5 shows the TEM and HRTEM images of cuboid-shaped TiO_2 NCs obtained with TBAH:DEA = 2:5 mol ratio. The size of these cuboid-shaped TiO_2 NCs varies in the range of 80–150 nm along diagonal (figures 5(a), (b)). Figure 5(c) shows the HRTEM image of an NC marked by the circle in figure 5(b). Figure 5(d) shows the magnified HRTEM image of the same NC showing the lattice fringes of 0.357 nm with an angle 84° clearly suggesting the $[11\bar{1}]$ zone axis and top facets of the NC with high-energy $\{001\}$ facets [27, 28]. Inset of 4(d) shows the corresponding FFT pattern further confirming the (101) and (011) planes along $[11\bar{1}]$ zone axis. Therefore, the top and bottom of the cuboids are of high-energy $\{001\}$ exposed facets. The FESEM analysis (figure 1(d)) and also TEM analysis (figures 5(a), (b)) reveal that the edges of the cuboid-shaped NCs are not sharp. The flattened edges of cuboid NCs are due to the low-energy $\{101\}$ exposed facets [15]. Moreover, the sides of the cuboids

body are high-energy $\{100\}/\{010\}$ facets as reported earlier [15].

Figure 6 shows the TEM and HRTEM images of TiO_2 NCs obtained with TBAH:DEA mol ratio of 1:10 at 225°C for 24 h. The shape of the TiO_2 NCs appears to be sheet-like and/or particle-like in a size range of 40–80 nm along the diagonal (figure 6(a)). Figure 6(b) shows the HRTEM image with the lattice fringe of 0.35 nm matching the (101) plane of anatase TiO_2 . The yellow colored arrow shows the growth along (101) plane with the high-energy $\{001\}$ exposed facets. In addition, the size of NCs is found to be smaller with a large quantity of DEA in the reaction medium (i.e. with TBAH:DEA = 1:10 mol ratio). From this we conclude that the mol ratio of TBAH:DEA plays an important role in forming diverse shapes of NCs. In particular, ellipsoid-shaped TiO_2 NCs are found majorly with $\{101\}$ exposed facets obtained with a smaller quantity of capping agent (i.e. with TBAH:DEA = 10:1 mol ratio). The rod- and capsule-shaped NCs are found with major $\{010\}$ exposed facets and minor $\{101\}$ exposed facets (for capsule-shaped NCs). The cuboid-shaped NCs are found to be equally exposed with $\{001\}$, $\{010\}$, and $\{101\}$ facets while sheet-like TiO_2 NCs are mainly exposed

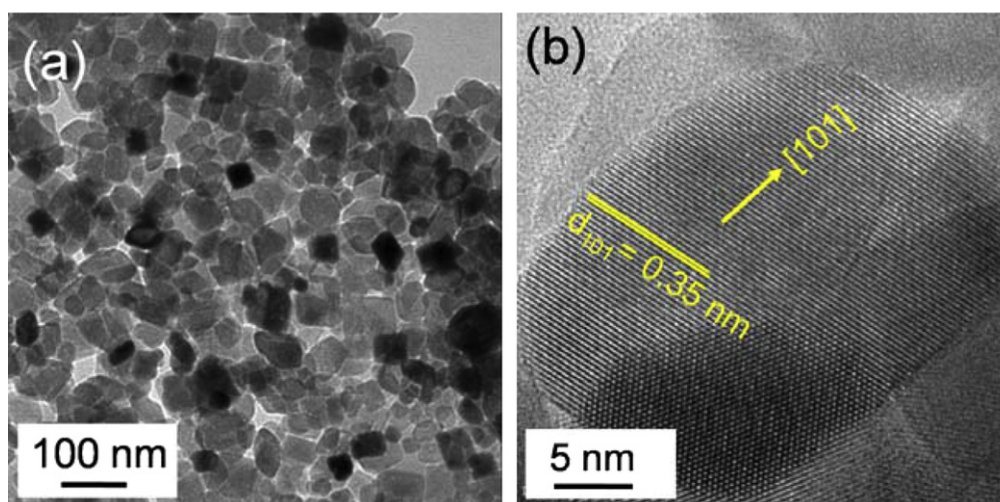


Figure 6. (a) TEM, and (b) HRTEM images of TiO₂ NCs obtained with TBAH:DEA = 1:10 with the reaction duration 24 h, reaction temperature 225 °C and TTIP precursor 3 mmol.

with {001} facets. The high-energy {001} exposed facets in the NCs are due to the hydrogen bonding of polar hydrogen of DEA with the consecutive 5c-Ti of {001} facets of TiO₂ during the course of crystal growth [15].

The FESEM and TEM analysis reveal the change in morphology of NCs by varying the mol ratio of DEA and TBAH with other reaction parameters fixed. During the formation of TiO₂ NCs, the growth normally occurs along *c*-axis producing tetragonal bipyramidal shape. The crystal growth can be tuned by employing suitable capping agent or facet terminating agent. In our previous work, we have shown that DEA acts as the capping agent which stabilizes the high-energy {001} facets through H-bonding [15]. Thus, growth along the *c*-axis is suppressed for NCs growth with a high DEA concentration and primary growth occurs along the *a*-axis producing sheet-like morphology with high-energy {001} exposed facets. With decrease in the DEA quantity, the capping along *c*-axis decreases and thereby growth along the thermodynamic direction, i.e. *c*-axis increases, which results in the formation of cuboid NCs, then capsule- and rod-shaped NCs.

The photocatalytic reactions are broadly divided into two classes: (i) catalyzed photoreactions are those where initial excitation occurs in an adsorbate molecule which then interacts with catalyst (adsorbent). (ii) Sensitized photoreactions are those where initial photoexcitation takes place on the catalyst surface and the photoexcited electrons/holes (e⁻/h⁺) take part in the reaction with adsorbate molecules [29]. Here the latter case is discussed, which normally involves formation of e⁻/h⁺ pairs in the semiconductor catalyst (such as TiO₂) under the light irradiation. The photoinduced e⁻ and h⁺ must efficiently travel to the surface of the catalyst in order to reduce and oxidize the adsorbate molecules, respectively. Thus, the process becomes efficient when species to be oxidized or reduced are preadsorbed on the catalyst surface and maximum charge separation (or recombination rate is low) occurs at the the catalyst surface. Furthermore, the rate of charge transfer (from catalyst to adsorbed species) depends on

the respective band edges of catalyst and redox potential of adsorbate species. This photocatalysis phenomenon has been extensively used for the degradation of several organic contaminants using TiO₂ as photocatalyst. The separated e⁻ and h⁺ react with the surface adsorbed water or oxygen to form hydroxyl radical and superoxide anion. Therefore, the photocatalytic activity of a catalyst is generally determined on the formation of OH[•] radical on the catalyst surface in the presence of charge carriers (electrons or holes) and water [5]. Although, the photocatalytic activity can be influenced by several factors such as the nature of surface adsorbed molecules and their electronic states, or with the nature of TiO₂ crystal facets, it has recently been reported that the {001} facets covered by water molecules show similar activity to those of {101} facets [30]. The OH[•] formation activity was tested using TA as the probe species. The TA reacts spontaneously with OH[•] producing hydroxylated TA (HTA), which shows a unique emission at ~430 nm [5]. The higher the formation of OH[•], the higher will be the HTA and thereby enhanced emission. Figure 7 shows the typical fluorescence spectra (measured in a fluorescence spectrophotometer, HITACHI F-7000) of HTA produced with different shapes of TiO₂ NCs catalyst (catalyst loading was 250 mg L⁻¹ mg in each case and catalyst was removed by centrifuging before the emission measurement of HTA) in 80 mL of 2 mM TA (in 0.1 M NaOH) aqueous solution irradiated under ultraviolet (UV) light for different durations. The emission intensity is found to increase with irradiation time for all the samples confirming the conversion of TA to HTA via the formation of OH[•] radical. The OH[•] is formed by the interaction of photo-generated electrons and holes with the adsorbed water or hydroxyl group on the catalyst surface [5].

Among the different shapes of TiO₂ NCs, rod-shaped TiO₂ NCs are found to be more active than the other shapes of TiO₂ NCs (figure 8). In spite of the larger size of the nanorods (figure 1(b), figure 4) and hence smaller BET surface area (~7 m² gm⁻¹) than the benchmark catalyst Degussa P25 (average size ~21 nm, specific surface area ~50 m² gm⁻¹),

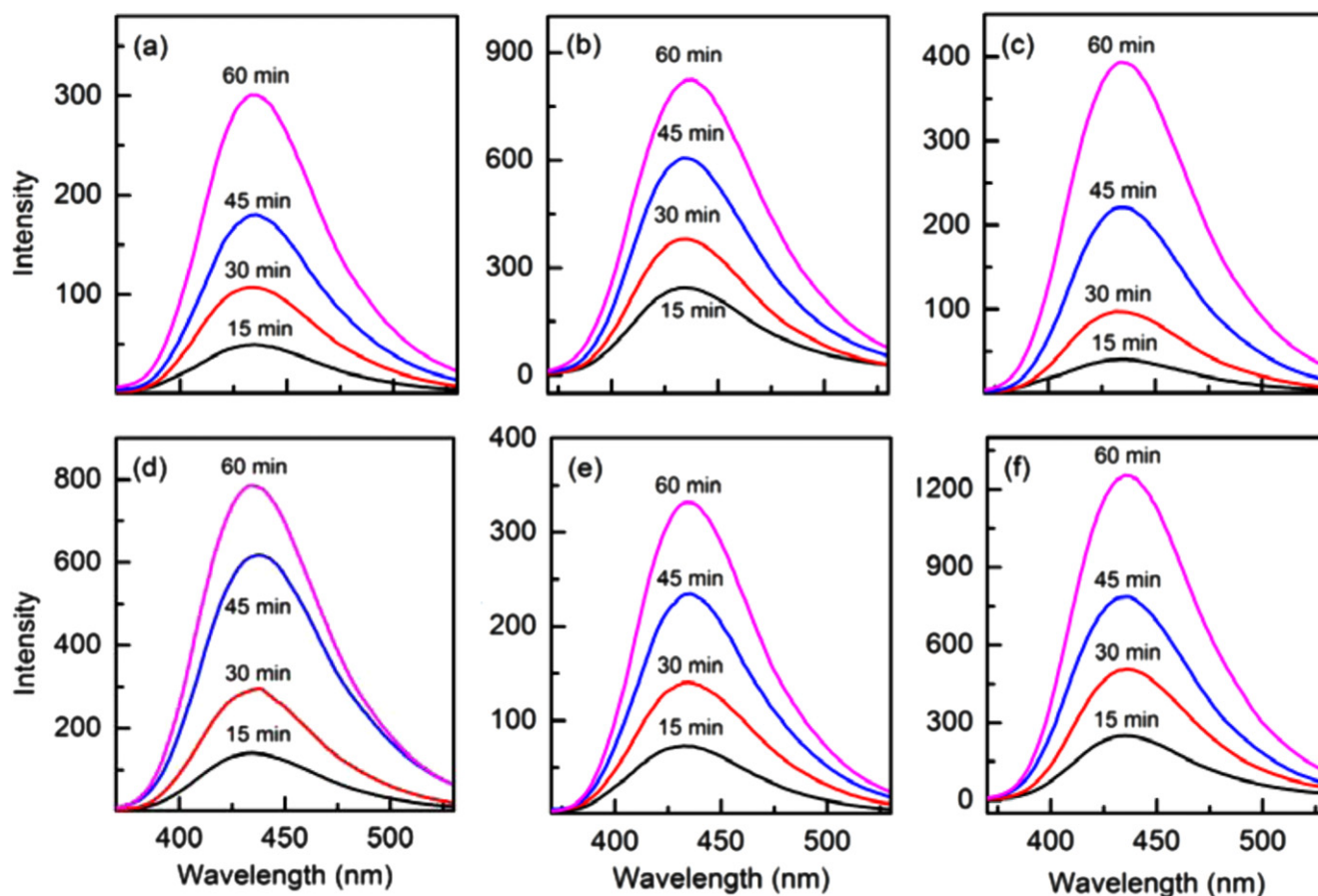


Figure 7. Fluorescence emission spectra of HTA at different UV irradiation time of 2 mM TA solution (in 0.1 M NaOH) in presence of (a) ellipsoid-shaped, (b) rod-shaped, (c) capsule-shaped, (d) cuboid-shaped, (e) sheet-like TiO_2 NCs, and (f) Degussa P25.

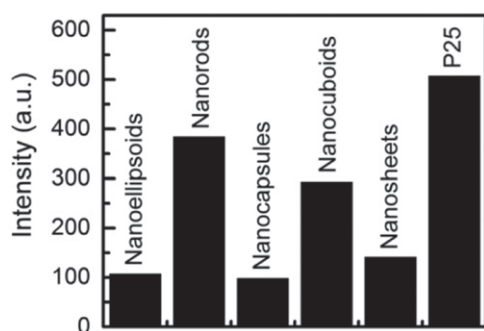


Figure 8. Emission intensity of HTA formed by different shapes of TiO_2 NCs and Degussa P25 in 30 min of UV light irradiation of 2 mM 0.1 M aqueous NaOH TA solution. The catalyst loading was 250 mg L^{-1} in each case.

nanorods show comparable OH^\bullet radical formation activity (figure 8). As the OH^\bullet radical formation takes place on the catalyst surface, specific surface area is important for the heterogeneous catalysis. Thus, we calculated the catalytic activity per specific surface area [5]. The activity per specific surface area towards the formation of OH^\bullet radical of TiO_2 nanorods is found to be >6 times higher than that of Degussa P25 and ~ 3 times higher than the cuboid-shaped TiO_2 NCs. The highest activity of the nanorods could therefore be ascribed to its major $\{010\}$ exposed facets. Although the sole

role of $\{010\}$ facets in the course of photocatalysis is not clear, the rod-shaped TiO_2 NCs have major $\{010\}$ and minor $\{101\}$ exposed facets. On the other hand, cuboid-shaped TiO_2 NCs have almost equal $\{001\}$, $\{010\}$ and $\{101\}$ exposed facets exhibiting lower catalytic activity than those of rod-shaped NCs. This indicates the maximum interaction between $\{010\}$ and $\{101\}$ facets with the photoexcited carriers which could decrease the recombination rate [18, 19].

4. Conclusions

Different shapes (ellipsoid, rod, capsule, cuboid and sheet-like) of TiO_2 NCs are synthesized by varying the mol ratio of TBAH and DEA using the hydrothermal growth technique. The sheet-like NCs are found with primarily high-energy $\{001\}$ exposed facets although the photocatalytic activity of the sheet-like TiO_2 NCs is poorer than the rod-shaped TiO_2 NCs, which is in accord with the theoretical prediction. The highest photocatalytic activity of rod-shaped TiO_2 NCs is ascribed to the presence of both high-energy $\{010\}$ and low-energy $\{101\}$ exposed facets, facilitating the charge carrier separation and therefore high rate of OH^\bullet radical formation.

Acknowledgments

This work was funded by the Department of Science and Technology, New Delhi, India (Indo—Korea/P-02) and National Research Foundation of Korea, MEST (NRF-2012R1A1A4A01005645). NR acknowledges CSIR, New Delhi for the financial support through CSIR scholarship.

References

- [1] Lazzeri M, Vittadini A and Selloni A 2001 *Phys. Rev. B* **63** 155409
- [2] Liu M, Piao L, Zhao L, Ju S, Yan Z, He T, Zhou C and Wang W 2010 *Chem. Commun.* **46** 1664–6
- [3] Yang H G, Sun C H, Qiao S Z, Zou J, Liu G, Smith S C, Cheng H M and Lu G Q 2008 *Nature* **453** 638–41
- [4] Tian F, Zhang Y, Zhang J and Pan C 2012 *J. Phys. Chem. C* **116** 7515–9
- [5] Yang H G, Liu G, Qiao S Z, Sun C H, Jin Y G, Smith S C, Zou J, Cheng H M and Lu G Q 2009 *J. Am. Chem. Soc.* **131** 4078–83
- [6] Selloni A 2008 *Nat. Mater.* **7** 613–5
- [7] Pan J, Liu G, Lu G Q and Cheng H–M 2011 *Angew. Chem., Int. Ed. Engl.* **50** 2133–7
- [8] Nguyen C K, Cha H G and Kang Y S 2011 *Cryst. Growth Des.* **11** 3947–53
- [9] Han X, Wang X, Xie S, Kuang Q, Ouyang J, Xie Z and Zheng L 2012 *RSC Adv.* **2** 3251–3
- [10] Han X, Zheng B, Ouyang J, Wang X, Kuang Q, Jiang Y, Xie Z and Zheng L 2012 *Chem.—Asian J.* **7** 2538–42
- [11] Vittadini A, Selloni A, Rotzinger F P and Grätzel M 1998 *Phys. Rev. Lett.* **81** 2954–7
- [12] Gong X–Q and Selloni A 2005 *J. Phys. Chem. B* **109** 19560–2
- [13] Jung M–A, Ko K C and Lee J Y 2014 *J. Phys. Chem. C* **118** 17306–17
- [14] Tachikawa T, Yamashita S and Majima T 2011 *J. Am. Chem. Soc.* **133** 7197–204
- [15] Roy N, Sohn Y and Pradhan D 2013 *ACS Nano* **7** 2532–40
- [16] Xing M–Y, Yang B–X, Yu H, Tian B Z, Bagwasi S, Zhang J–L and Gong X–Q 2013 *J. Phys. Chem. Lett.* **4** 3910–7
- [17] Selcuk S and Selloni A 2013 *J. Phys. Chem. C* **117** 6358–62
- [18] Nunzi F, Storchi L, Manca M, Giannuzzi R, Gigli G and Angelis F D 2014 *ACS Appl. Mater. Interfaces* **6** 2471–8
- [19] Ma X, Dai Y, Guo M and Huang B 2013 *Langmuir* **29** 13647–54
- [20] Diebold U 2003 *Surf. Sci. Rep.* **48** 53–229
- [21] Kumar S G and Devi L G 2011 *J. Phys. Chem. A* **115** 13211–41
- [22] Wang D, Kanhere P, Li M, Tay Q, Tang Y, Huang Y, Sum T C, Mathews N, Sritharan T and Chen Z 2013 *J. Phys. Chem. C* **117** 22894–902
- [23] Maitani M M, Tanaka K, Mochizuki D and Wada Y 2011 *J. Phys. Chem. Lett.* **2** 2655–9
- [24] Angelis F D, Valentin C D, Fantacci S, Vittadini A and Selloni A 2014 *Chem. Rev.* **114** 9708–53
- [25] Wang Z, Lv K, Wang G, Deng K and Tang D 2010 *Appl. Catal. B* **100** 378–85
- [26] Zhu J, Wang S, Bian Z, Xie S, Cai C, Wang J, Yang H and Li H 2010 *Cryst. Eng. Comm.* **12** 2219–24
- [27] Patra A K, Dutta A and Bhaumik A 2014 *J. Phys. Chem. C* **118** 16703–9
- [28] Ding K, Miao Z, Liu Z, Zhang Z, Han B, An G, Miao S and Xie Y 2007 *J. Am. Chem. Soc.* **129** 6362–3
- [29] Linsebigler A L, Lu G and Yates J T 1995 *Chem. Rev.* **95** 735–58
- [30] Li Y–F and Liu Z–P 2011 *J. Am. Chem. Soc.* **133** 15743–52